European Association for the Development of Renewable Energies, Environment and Power Quality (EA4EPQ)

International Conference on Renewable Energies and Power Quality (ICREPQ'12)
Santiago de Compostela (Spain), 28th to 30th March, 2012

Modelling of Photovoltaic Generators Based on a Linarized Equivalnet Circuit

Andreas D. Theocharis[1,2], Eleftheria C. Pyrgioti[2], Ioannis A. Naxakis[2]

[1] Department of Electrical Engineering
Technological and Educational Institute of Patras
1 M. Alexandrou, Koukouli, 26334 Patras (Greece)

[2] Department of Electrical and Computer Engineering
University of Patras
University Campus, Rion, 26500 Rion (Greece)
E-mail: theoxar@ece.upatras.gr, E.Pyrgioti@ece.upatras.gr, naxakis@ece.upatras.gr

Abstract. In this paper, a new method on modeling of PV generators, for association with electromagnetic software programs, is proposed. The application of a linearization process, on nonlinear and well-tested current-voltage equations using Taylor's scheme, leads to uncoupling of the current and voltage quantities in each time step of a digital simulation. This uncoupling is represented by a linearized equivalent electrical circuit. Using the proposed equivalent photovoltaic generator circuit, the application of nodal analysis on equivalent resistive circuits derives a photovoltaic system model of linear algebraic equations. This remarkably simplifies photovoltaic systems modeling because one can develop a photovoltaic generator element in electromagnetic transient programs for power systems analysis.

Key words

Photovoltaics, nonlinear circuits, power generation.

1. Introduction

In order to conduct performance studies on intergraded photovoltaic (PV) systems, measurements on operating installations [1] and digital simulations are used. In general, digital simulations have the advantage in comparison to measurements because they are fast, without cost as well as give the opportunity for sensitivity analysis on various design parameters. In these studies, the interest is focused on the upgrade of the models of the individual units of a PV system [2-4] as well as on the control aspects of the PV system in order to operate with high efficiency [5-7] and under maximum power conditions [8-12].

Digital power system simulations studies are conducted using electromagnetic transient software programs which are based on nodal analysis on equivalent resistive circuits [2], [4] and [13-17]. Many nonlinear PV generator models have been used to describe PV generators. They cannot directly be involved within electromagnetic transient software programs because their usage leads to nonlinear node equations. Therefore, PV generator's modeling, using these software programs, is accomplished by two methods. In the first method, one has to develop from the beginning a suitable PV generator model by designing a block-circuit using several elements and control commands. This task may be of the same level of complexity as the study of the whole PV system. In the second method, one can approximate the nonlinear PV characteristic curve by a piecewise linearized one. Consequently, their usage leads to piecewise linearized node equations. An extended review one can find in [4].

In this paper, a new linearized equivalent circuit model of PV generators is proposed. The presented model is based on linearization of a authoritative nonlinear initial $i_{pv}(v_{pv})$ equation using Taylor's scheme. The process leads to uncoupling of the i_{pv}-v_{pv} electrical quantities in each time step Δt of a digital simulation. This uncoupling can be represented by an equivalent linearized current source in parallel with a linearized ohmic resistance. Applications of the proposed model, involving equivalent resistive circuits of lumped L and C elements, show that it can be associated with electromagnetic transient software packages based on node equations. Moreover, it can be combined with suitable models of other nonlinear units of a PV system, in order to perform sensitivity analysis studies.

2. Model Development

It is assumed that at time t_0 the voltage and the current of the PV generator have values $v_{pv}(t_0)$ and $i_{pv}(t_0)$, respectively. If Δt is the time step of the simulation, it is assumed that at time instant $t=t_0+\Delta t$ the operation point has values $v_{pv}(t)$ and $i_{pv}(t)$, respectively. An initial $i_{pv}(v_{pv})$

nonlinear equation is supposed which can be approximated by a Taylor series in the space $[v_{pv}(t_0), v_{pv}(t)]$ evaluating the expression at $v_{pv}(t_0)$

$$i_{pv}\ t\ = i_{pv}\ t_0\ + \left.\frac{di_{pv}}{dv_{pv}}\right|_{\left[v_{pv}\ t_0\ \right]} \left[v_{pv}\ t\ - v_{pv}\ t_0\ \right] + \left.\frac{d^2 i_{pv}}{dv^2{}_{pv}}\right|_{\left[v_{pv}\ t_0\ \right]} \left[v_{pv}\ t\ - v_{pv}\ t_0\ \right]^2 + ... \quad (1)$$

By neglecting the second-order and higher-orders of the difference $\left[v_{pv}\ t\ - v_{pv}\ t_0\ \right]$, keeping only the first two terms in (1) and due to the fact that $\left.\frac{di_{pv}}{dv_{pv}}\right|_{\left[v_{pv}\ t_0\ ,i_{pv}\ t_0\ \right]} \langle 0$ one arrives at the following expression

$$i_{pv}\ t\ = i_{pv}\ t_0\ - \frac{1}{r_{pv0}}\left[v_{pv}\ t\ - v_{pv}\ t_0\ \right] \quad (2)$$

where r_{pv0} is defined as the incremental resistance at the point $\left[v_{pv}\ t_0\ ,i_{pv}\ t_0\ \right]$

$$r_{pv0} = \left[-di_{pv}/dv_{pv}\Big|_{\left[v_{pv}\ t_0\ ,i_{pv}\ t_0\ \right]}\right]^{-1} \quad (3)$$

By rearranging the terms in (2), one can write

$$i_{pv}\ t\ = I_0 - \frac{v_{pv}\ t}{r_{pv0}} \quad (4)$$

where

$$I_0 = i_{pv}\ t_0\ + \frac{v_{pv}\ t_0}{r_{pv0}} \quad (5)$$

Equation (4) gives the position of the operation point of the PV generator on the i_{pv}-v_{pv} plane at the time instant $t=t_0+\Delta t$ using values from the previous time instant t_0. Thus, one can predict the trajectory of the operation point of the PV generator at any time instant $t=t_0+\Delta t$ using the tangent on the initial nonlinear v_{pv}-i_{pv} curve at the time instant t_0 by properly updating the parameters I_0 and r_{pv0} in each time interval Δt. This is represented by the equivalent circuit in Fig.1 in the time interval Δt.

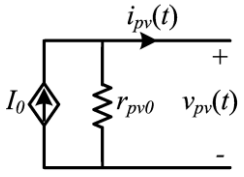

Fig. 1 The equivalent linearized circuit of the PV generator at the time instant $t=t_0+\Delta t$.

The calculation of the parameter r_{pv0} is based on the calculation of the derivative of the current i_{pv} with respect to the voltage v_{pv} by using the initial nonlinear $i_{pv}(v_{pv})$ equation. In this paper, the authoritative and well known nonlinear curves given in the Appendix by equations (10) and (11), are used. Applying (3) on (10) and (11) one derives that r_{pv0} is given by

$$r_{pv0} = 1\Big/\ I_{sc}k_1k_2m\left[v_{pv}\ t_0\ \right]^{m-1} e^{k_2\left[v_{pv}\ t_0\ \right]^m} \quad (6)$$

for the first model and r_{pv0} is given by

$$r_{pv0} = \frac{1+Wr_s\left[I_{ph}+I_D-i_{pv}\ t_0\ \right]}{W\left[I_{ph}+I_D-i_{pv}\ t_0\ \right]} \quad (7)$$

using the second model. Except of equations (10) and (11), other suitable initial $i_{pv}(v_{pv})$ exponential equations can be used [15] and [18, 19].

3. Results

A. Verification of the model using a PVrLC circuit

The *PVrLC* circuit in Fig. 2(a), using the equivalent circuit of the PV generator in Fig. 1 and the equivalent resistive circuits for the *L* and *C* elements given in [30], has the equivalent resistive circuit in Fig. 2(b).

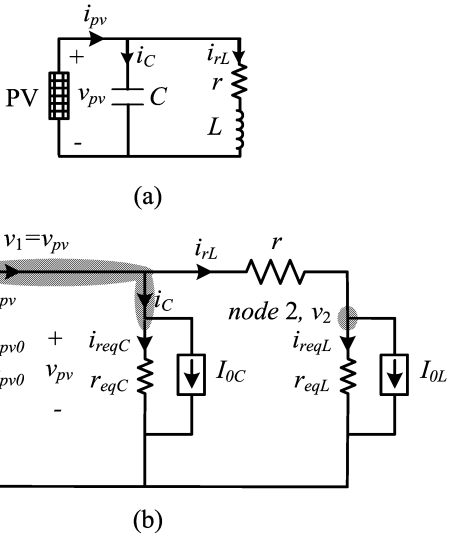

Fig 2. An *rLC* circuit energized by a *PV* generator: (a) the equivalent circuit using lumped *L* and *C* elements, (b) the equivalent resistive circuit.

In view of Fig. 2(b), the corresponding state vector is $v_1\ \ v_2\ ^{\mathrm{T}}$. Applying node equations, the system of the linear algebraic equations in (8) governs the circuit in Fig. 2(b)

$$\begin{bmatrix} r_{pv0}+r^{-1}+r_{eqC}^{-1} & -r^{-1} \\ r^{-1} & -r^{-1}-r_{eqL}^{-1} \end{bmatrix}\begin{bmatrix} v_1 \\ v_2 \end{bmatrix} = \begin{bmatrix} I_o - I_{0C} \\ I_{0L} \end{bmatrix} \quad (8)$$

where r_{pv0} can be given by (6). Equation (8) is solved assuming initial conditions $v_1\ t=0\ =0$ and $v_2\ t=0\ =0$. The transient response of the circuit is shown in Fig. 3(a) using the values shown in Table I. Moreover, the trajectories for the time interval from $t=0$ to steady state on i_{pv}-v_{pv} and P_{pv}-v_{pv} planes are shown in Fig. 3(b) and Fig. 3(c), respectively, for different levels of insolation and temperature. The predicted i_{pv}-v_{pv} and P_{pv}-v_{pv} curves, using the equivalent circuit of the PV generator, are in excellent agreement with the measured values and consequently, the linearized model successfully can predict the nonlinear performance of a PV generator.

Table I.- Data for the simulation of the *PVrLC* circuit

PV Generator [20]		*rLC*
P_{pv}=110 W	a_t=1.4 mA/^{o}C	
I_{mpp}=3.15 A	b_{oc} =-152 mV/^{o}C	r=122.592 Ω
V_{mpp}=35 V	P_{mpp}=110 W	L=10 mH
I_{sc}=3.45 A	V_{oc}=43.5 V	C=0.1 mF
G=900 W/m^2	T_a=35 ^{o}C	$\Delta t=10^{-5}$ sec

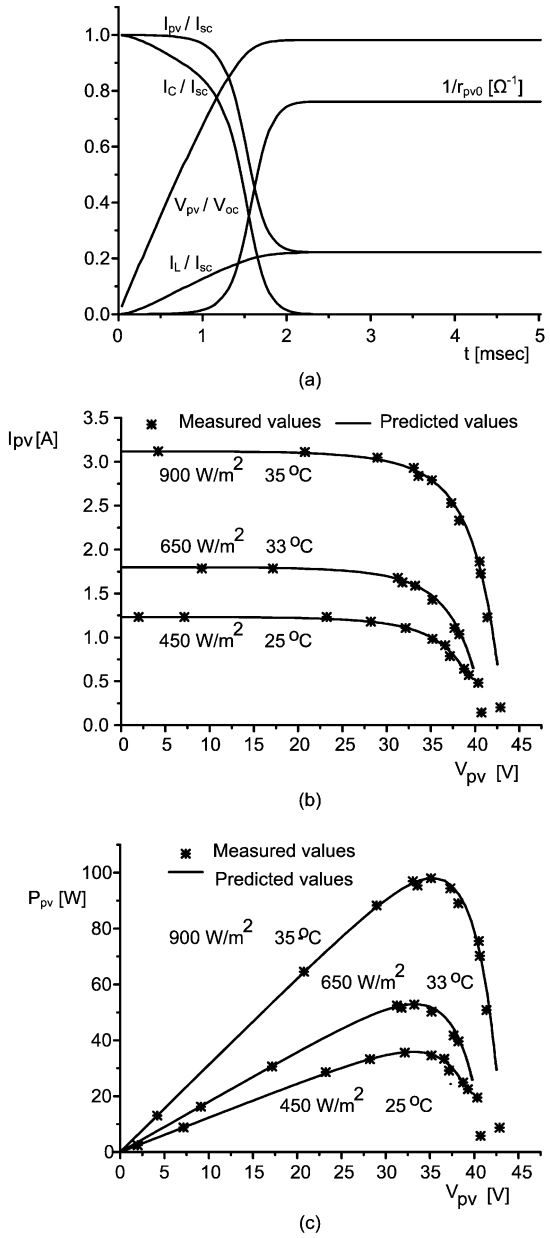

Fig 3. The transient response of the PVrLC circuit in Fig. 2: (a) voltage and current waveforms from t=0 to steady state, (b) the measured and predicted i_{pv}-v_{pv} curves for different levels of insolation and temperature, (c) the measured and predicted P_{pv}-v_{pv} curves for different levels of insolation and temperature

B. Modeling and simulation of a grid connected PV system

A simplified configuration of a grid connected PV system includes a PV generator, a dc filter, a dc-ac inverter, an isolation transformer and the utility grid. Such an installation is shown in Fig. 4(a), using lumped parameters. The PV generator is presented by its equivalent circuit in Fig. 1 and using (7) for the calculation of r_{pv0}, the isolation transformer is referred at the PV generator side and it is represented by a linear equivalent inductance L_{tr}/a_{tr}^2 for both primary and secondary sides. A simplified representation of the single-phase inverter is considered where all switching devices are modeled as ideal switches, implying zero resistance when closed and infinite resistance when open. Moreover, the inverter operates with none or two switches conducting.

In Fig. 4(b) the topology of the grid connected PV system is shown when switches ″1″ and ″2″ are closed and switches ″3″ and ″4″ are open. The corresponding equivalent resistive circuit is presented in Fig. 4(c). In this case, the state variables of the system are $\begin{bmatrix} v_1 & v_2 \end{bmatrix}^T$ and applying node equations one can easily derive the state equations of the grid connected PV system which are

$$\begin{bmatrix} 1/r_{eq.Lt} & 1/r_{pv0}+1/r_{eq.C} \\ -1 & 1 \end{bmatrix} \begin{bmatrix} v_1 \\ v_2 \end{bmatrix} = \begin{bmatrix} I_0 - I_{0Lt} - I_{0C} \\ e_g / a_{tr} \end{bmatrix} \quad (9)$$

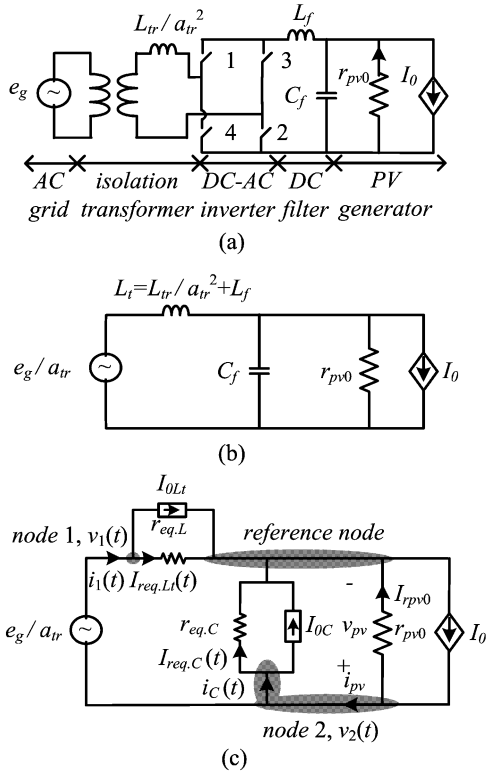

Fig. 4. A grid connected PV system: (a) Typical configuration where the transformer is referred at the PV generator side with transformation ratio a_{tr}, (b) System topology, when switches ″1″ and ″2″ are closed and switches ″3″ and ″4″ are open, using equivalent r, L and C elements where $L_t=L_{tr}/a_{tr}^2+L_f$, (c) The equivalent resistive circuit of the system in (b).

Primary simulation results, using the data in Table II of a prototype system located in Phoenix Arizona [21], are shown in Fig.5. By calculating the firing angle of the inverter, the voltage of the PV generator is adjusted, in both cases of the value of the insolation, at about 190V. When insolation is decreased from 0.55kW/m^2 to 0.40kW/m^2, the system passes to non-continuous conduction mode as it shown in Fig 5(a) and Fig. 5(d).

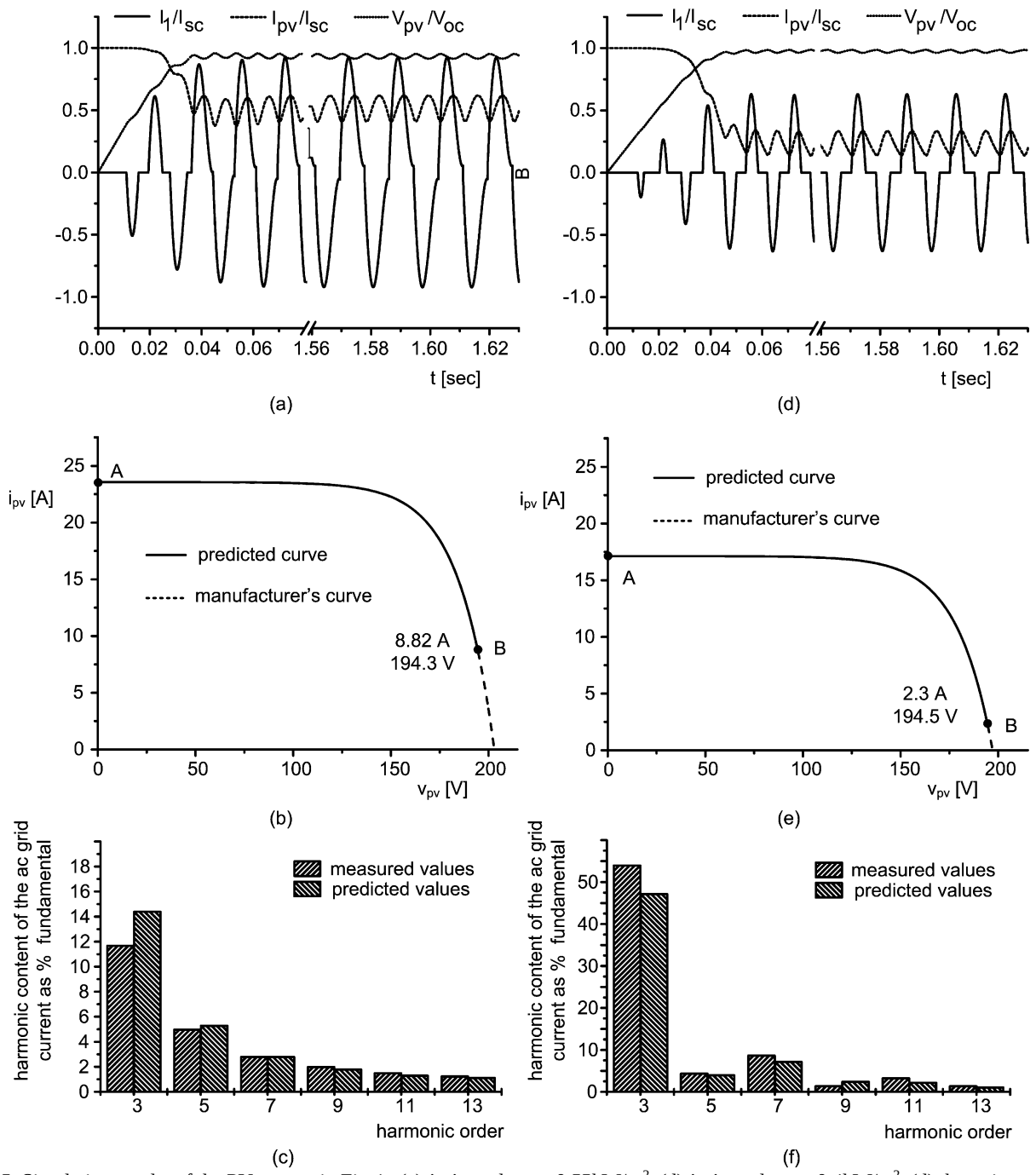

Fig. 5. Simulation results of the PV system in Fig 4:, (a) i_1, i_{pv} and v_{pv} at 0.55kW/m^2, (d) i_1, i_{pv} and v_{pv} at 0.4kW/m^2, (d) the trajectory on the i_{pv}-v_{pv} plane in the time interval from t=0 until the current i_{pv} takes its minimum value at 0.55kW/m^2, (e) the trajectory on the i_{pv}-v_{pv} plane in the time interval from t=0 until the current i_{pv} takes its minimum value at 0.4kW/m^2, (c) the measured and predicted values the harmonic content of the injected current into the ac grid at 0.55kW/m^2, (f) the measured and predicted values the harmonic content of the injected current into the ac grid at 0.4kW/m^2

Table II.- Data for the simulation of the grid connected PV system [21]

ac Grid	Transformer	Dc filter	PV Generator
Frequency 60 Hz	L_{tr} 320 μH	L_f 25 mH	W 0.54932 V^{-1}
RMS voltage 240 V	a_{tr} 1	C_f 3.3 mF	r_s 2.15 mΩ
			v_{pv} 190V
			I_{ph} (0.55 kW/m^2) 23.562 A
			I_{ph} (0.40 kW/m^2) 17.136 A

This is because the current of the PV generator has decreased, as it is shown in Fig. 5(b) and Fig. 5(e), where the trajectories of the operating points on the i_{pv}-v_{pv} plane are drawn in the time interval from t=0 until the current i_{pv} takes its minimum value. Moreover, as it was expected, the predicted i_{pv}-v_{pv} curves, using the proposed equivalent circuit of the PV generator, coincide with the i_{pv}-v_{pv} curves given by the manufacturer which are calculated using (11).

Regarding the harmonic content of the injected current into the ac grid, the measured and predicted values are shown in Fig. 5(c) and 5(f). It is observed high value of

the third harmonic at 0.40kW/m^2 in comparison with the value of the third harmonic at 0.55kW/m^2 because the inverter operates in non-continuous conduction mode. Furthermore, comparing the results for the third harmonic, which dominates, the errors between the measured and predicted values are about 22.7% (0.55kW/m^2) and 12.68% (0.40kW/m^2). These errors are due to the fact that the inverter is considered as ideal component and the transformer is considered as linear unit. In general, further agreement between measured and predicted values could be achieved if accurate models for the inverter and the transformer are used.

The performance of the system in Fig. 5 does not correspond to a well designed commercial grid connected photovoltaic system, using the parameters in Table II Specifically, concerning the THD of the injected, into utility grid, current i_1, at 0.55kW/m^2 the THD is 0.16 while at 0.4kW/m^2 the THD is 0.48. A short sensitivity investigation, on the TDH of the injected current i_1 with parameters the values of the DC filter has been conducted at 0.4kW/m^2.

The results show that the size of the capacitor C_f does not affect THD of the injected current i_1, as expected due to the fact that a capacitor affects voltage waveform. Figure 6 shows the performance of the system by varying the inductor size from 10mH up to 300mH. As shown in Fig. 6, in the range 10mH up to 120mH (approximately) the inverter operates in non-continuous conduction mode and, THD rapidly decreases. This is due to the fact the 3rd harmonic dominates in this conduction mode of the inverter in comparison to the 5th harmonic and rapidly is decreased. In the range 120mH (approximately) up to 300mH, the inverter operates in continuous conduction mode, which means that the waveshape of i_1 has a tendency to become a square wave and THD increases. An extended, and more detailed, sensitivity analysis has to be based on more accurate models for the inverter and isolation transformer.

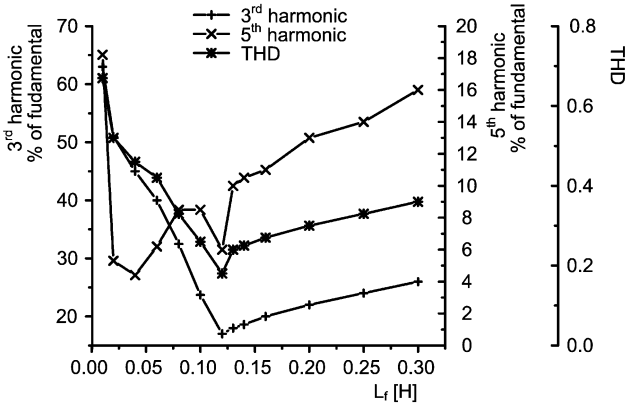

Fig. 6. The performance of the system in Fig. 4 by varying the inductor size from 10mH up to 300mH (C_f=3.3mF, v_{pv} =190V)

4. Conclusions

A linearized equivalent electrical circuit of a PV generator is presented which is derived from the linearization of authoritative nonlinear $i_{pv}(v_{pv})$ equations using Taylor series. The linearized equivalent circuit is represented by a dependent current source I_0 in parallel with a variable resistance r_{pv0}, both updated in each time interval Δt.

The applications and the simulation results show that using typical values of the time step, excellent numerical stability has been observed as well as excellent agreement, between measured values and predicted values at different conditions of temperature and insolation, has been achieved. Furthermore, the proposed linearized circuit model can be associated with several electromagnetic transient software packages, based on nodal, analysis simplifying the introduction of a PV generator in an electromagnetic transient software package.

At this point, it should be noted that any improvements on the equations used to calculate parameters of the initial nonlinear models, such as k_1, k_2, k_3, k_4, m, I_{ph} and I_D [22, 23] can be included without restricting or influencing the simplicity of the procedure. The proposed technique can also be applied on other initial nonlinear $i_{pv}(v_{pv})$ characteristic equations [18, 19, 24-27] which will simply result in a different equation for the incremental resistance r_{pv0}. Future work in this area includes the analytical implementation of the proposed circuit into most commonly used commercial programs.

5. Appendix

In order to describe the method, two different nonlinear authoritative and published models of a PV generator have been selected. The first model is based on an exponential type equation involving four parameters [20], which, under Standard Test Conditions (STC), is represented by the equation

$$i_{pv} = I_{sc}\left[1 - k_1\left(e^{k_2 v_{pv}^m} - 1\right)\right] \tag{10}$$

The coefficients k_1 up to k_4 and m are defined through equations given in [20] which are given in relation to V_{mpp} the maximum power point voltage, I_{mpp} the maximum power point current, V_{oc} the open circuit voltage and I_{sc} the short circuit current. The above defined i_{pv}-v_{pv} curve can be used as a reference curve. In the case of different conditions of insolation and temperature, new characteristic curve can be determined using the relations given [20] which are based on G_r the solar insolation under reference conditions, a_r the current-temperature coefficient, I_{scr} the short-circuit current under reference conditions, b_{oc} the voltage-temperature coefficient, r_s the series resistance and T_r the temperature under reference conditions. The second PV model is based on a combination of the *i-v* characteristic curve of a simple diode equivalent model [28]. The following mathematical expression describes the PV generator under insolation G and temperature T_a

$$i_{pv} = I_{ph} - I_D\left[e^{W\,v_{pv}+i_{pv}r_s} - 1\right] \tag{11}$$

where the light-generated current I_{ph} and the diode saturation current I_D can be determined from values under STC [16], [29] using the equations

$$I_{ph} = \left[I_{scr} + a_r \ \ T_a - T_r \ \right] G/G_r \quad (12)$$

$$I_D = I_{Dr} \left(\frac{T_a}{T_r} \right)^3 e^{\left[\frac{E_{GO}}{fK} \left(\frac{1}{T_r} - \frac{1}{T_a} \right) \right]} \quad (13)$$

respectively, where *f* is an experimentally defined constant appropriate for the agreement between (11) and experimental values, I_{Dr} is the diode saturation current under reference conditions and E_{GO} the energy gap of the semiconductor. Moreover, the term *W* is given by

$$W = {}^{q}\!/_{wKT_a} \quad (14)$$

where *q* is the electron charge, *w* is a curve fitting constant and *K* is the Boltzmann's constant.

References

[1] Vokas, G. A., and Machias, A. V.: 'Harmonic voltages and currents on two Greek islands with photovoltaic stations: study and field measurements', IEEE Transactions on Energy Conversion, 1995, 10, (2), pp. 302-306

[2] Wang, Y.-J., and Hsu, P.-C.: 'Analytical modelling of partial shading and different orientation of photovoltaic modules', IET Renewable Power Generation, 2010, 4, (3), pp. 272-282

[3] Long, X., Liao, R., and Zhou, J.: 'Low-cost charge collector of photovoltaic power conditioning system based dynamic DC/DC topology', IET Renewable Power Generation, 2011, 5, (2), pp. 167-174

[4] Wang, Y.-J., and Hsu, P.-C.: 'Modelling of solar cells and modules using piecewise linear parallel branches', IET Renewable Power Generation, 2011, 5, (3), pp. 215-222

[5] Bowtell, L., and Ahfock, A.: 'Direct current offset controller for transformerless single-phase photovoltaic grid-connected inverters', IET Renewable Power Generation, 2010, 4, (5), pp. 428-437

[6] Delfino, F., Procopio, R., Rossi, M., and Ronda, G.: 'Integration of large-size photovoltaic systems into the distribution grids: a P–Q chart approach to assess reactive support capability', IET Renewable Power Generation, 2010, 4, (4), pp. 329-340

[7] Karatepe, E., Syafaruddin, and Hiyama, T.: 'Simple and high-efficiency photovoltaic system under non-uniform operating conditions', IET Renewable Power Generation, 2010, 4, (4), pp. 354-368

[8] Abd El-Shafy A. Nafeh, Fahmy, F. H., and Abou El-Zahab, E. M.: 'Maximum power point operation of a stand-alone system using fuzzy logic control', International Journal of Numerical Modelling, 2002, 15, pp. 385-398

[9] Salas, V., Olias, E., Barrado, A., and Lazaro, A.: 'Review of the maximum power point tracking algorithms for stand-alone photovoltaic systems', Solar Energy Materials and Solar Cells, 2006, 90, pp. 1555-1578

[10] Kyritsis, A. Ch., Tatakis, E. C., and Papanikolaou, N. P.; Optimum design of the current-source flyback inverter for decentralized grid-connected photovoltaic systems', IEEE Transactions on Energy Conversion, 2008, 23, (1), pp. 281-293

[11] Piegari. L., and Rizzo, R.: 'Adaptive perturb and observe algorithm for photovoltaic maximum power point tracking', IET Renewable Power Generation, 2010, 4, (4), 317-328

[12] Andrejasic, T., Jankovec, M., and Topic, M.: 'Comparison of direct maximum power point tracking algorithms using EN 50530 dynamic test procedure', IET Renewable Power Generation, 2011, 5, (4), pp. 281-286

[13] Ho, F. D., and Morgan, T. D.: 'SPICE modeling of cascade solar cells', IEEE Proceedings of Southeastcon '91, 1991, 2, pp. 776-780.

[14] Zerky, A., and Al-Mazroo, A. Y.: 'A distributed SPICE-model of a solar cell', IEEE Transactions on Electron Devises, 1996, 43, (5), pp. 691-700

[15] Gow, J. A.,and Manning, C. D.: 'Development of a photovoltaic array model for use in power electronics simulation studies', IEE Proceedings on Electric Power Applications, 1999, 146, (2), pp. 193-200

[16] Chao, K. H., Ho, S. H., Wang, M. H.: 'Modeling and fault diagnosis of a photovoltaic system', Electric Power Systems Research, 2008, 78, pp. 97-105

[17] Cho, H. I., Yeo, S. M., Cim, C. H., Terzijia, V., and Radojevic, Z. M.: 'A Steady-State Model of the Photovoltaic System in EMTP', International Conference on Power Systems Transients (IPST2009), Kyoto, Japan, June 3-6, 2009

[18] Saetre, T. O., Midtgard, O.-M., Yordanov, G.-H.: 'A new analytical solar cell I-V curve model', Renewable Energy, 2011, 36, pp. 2171-2176

[19] Di Piazza, M.-C., Vitale, G.: 'Photovoltaic field emulation including dynamic and partial shadow conditions', Applied Energy, 2010, 87, pp. 814–823

[20] Lalouni, S., Rekioua, D., Rekioua, T., and Matagne, E.: 'Fuzzy logic control of stand-alone photovoltaic system with battery storage', Journal of Power Sources, 2009, 193, pp. 899-907

[21] Mc Neill B., and Mizra M.: 'Estimated Power Quality for Line Commutated Photovoltaic Residential System', IEEE Transactions on Power Applications and Systems, 1983, PAS-102, (10), pp. 3288-3295

[22] De Soto, W., Klein, S. A., Beckman, W. A.: 'Improvement and validation of a model for photovoltaic array performance, Solar Energy, 2006, 80, pp. 78-88

[23] Lo Brano, V., Orioli, A., Ciulla, G., and Di Gangi, A.: 'An improved five parameter model for photovoltaic modules', 2010, Solar Energy Materials & Solar Cells, 94, pp. 1358-1370

[24] Akbaba, M., Alattawi, M. A. A.: 'A new model for I-V characteristic of solar cell generators and its applications, Solar Energy Materials and Solar Cells, 1995, 37, pp. 123-132

[25] Khouzam, K, and Hoffman, K.: "Real-time simulation of photovoltaic modules', Solar Energy, 1996, 56, (6), pp. 521-526

[26] Garrido-Alzar, C. L.: 'Algorithm for extraction of solar cell parameters from I-V curve using double exponential model, Renewable Energy, 1997, 10, pp. 125-128

[27] Elshatter, Th. F., Elhagry, M. T., Abou-Elzahab, E. M., and Elkousy, A. A. T.: 'Fuzzy modeling of photovoltaic panel equivalent circuit, Proceedings of the Photovoltaic Specialists Conference, 2000, 15, (22), pp. 1656-1659

[28] Garcia-Valverde, R., Miguel, C., Martinez-Bejar, R., and Urbina, A.: 'Optimized photovoltaic generator electrolyser coupling through a controlled DC-DC converter', International Journal of Hydrogen Energy, 2008, 33, pp. 5352-5362

[29] Thai, H. L., Tu, C. S., and Su, Y. J.: 'Development of generalized photovoltaic model using Matlab/Simulink', Proceedings of the World Congress on Engineering and Computer Science, WCECS 2008, USA 2008.

[30] Dommel H.W.: 'Linear uncoupled lumped elements', in 'ElectroMagnetic Transients Programm Reference Manual (EMTP Theory Book)' (Bonneville Power Administration, Portland, USA, 1986), pp. 2-31.